

## XII. SOOT FORMATION IN A TURBULENT SWIRLING FLOW

David P. Hault

Massachusetts Institute of Technology  
Department of Mechanical Engineering

In a gas turbine combustor, fuel and air are fed separately and combustion occurs primarily within a spacially limited zone. Turbulent mixing rates in such a system have important effects on the emission of pollutants such as nitric oxide, carbon monoxide, and soot. This report summarizes the qualitative understanding of soot formation in simple models of gas turbine primary-zone combustors.

Soot formation is important in flame radiation and air pollution. Knowledge of the concentration of soot particles is necessary to predict flame emissivities for radiative heat transfer problems. Also, some carcinogens are associated with soot particles. Because small soot particles may be deposited deep in the lungs, they may be hazardous to human health. Oxides of nitrogen ( $\text{NO}_x$ ) control strategies, such as lower temperature and/or staged combustion tend to increase soot formation (ref. 1). The use of highly aromatic fuels such as those made from coal would increase attention on soot because these fuels, in some geometries, tend to generate more soot than conventional fuels.

Little is known about turbulent diffusion flames in geometries approximating elements of gas turbine combustors. After being surprised by many of our results, we are confident of only a few general statements: First, if the fuel is premixed with air in approximately stoichiometric proportions, the sequence of states that a fluid element undergoes as it burns is quite different from the sequence when liquid or vapor fuel is injected into an air-flow. Second, swirling flows, as are typical of swirl-can combustors, when burning, can amplify small aerodynamic disturbances upstream of the swirl vanes. Third, different fuels form significantly different amounts of soot. Each of these effects makes major changes in the amount of soot formed in a given combustor.

## BURNERS

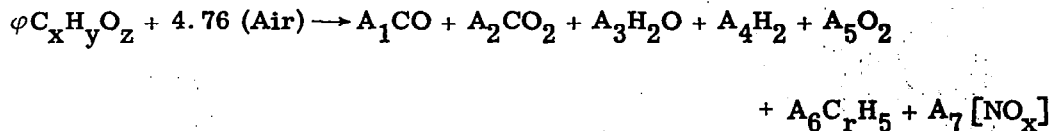
The burners used consist of cylindrical insulated tubes, 3 inches in diameter, in one end of which is mounted a 45<sup>0</sup>-blade-angle swirler and an air-assist atomizer (DeLavan model 30609-11) on the axes of symmetry. The atomizer airflow is about 5 percent of the total airflow. Although this sounds straightforward enough, the aerodynamics of such simple systems cannot be specified because of hardware effects upstream of the swirler and atomizer.

Gas and soot samples were collected at different flame positions with a stainless-steel, water-cooled probe (fig. XII-1) that was developed by Dr. Gilles Prado of the Centre des Recherches sur la Physico-Chimie des Surface Solides, Mulhouse, France. With this probe, one can sample either gases (CO, CO<sub>2</sub>, hydrocarbons, NO<sub>x</sub>, and O<sub>2</sub>) or soot. When gases are collected, the probe is adjusted so that it is water cooled, but no water mixes with the quenched gas samples. When soot is collected, the probe is water flushed, and the soot is collected on a fiber-glass filter, from which it is extracted and weighed. Details of the soot-measuring method are given in reference 1. Reproducibility of soot concentrations is about 10 percent. Because of the rapid quenching in the probe (in about 10<sup>-4</sup> sec), reactions between water and soot can be ignored. We have reported the experiment over a range of water flush and collection velocities and operate the experiment in a state where the amount of soot does not depend on either the water velocity or the gas collection agency.

## PRELIMINARY RESULTS

Figure XII-2 shows the original burner. Although it looks quite straightforward, it is not. The difficulty comes in trying to describe the aerodynamic effects of the fittings that connect to the atomizer.

The gas constituents as well as soot were measured. Figure XII-3 describes the method used. In particular, when concentrations of CO, CO<sub>2</sub>, hydrocarbons, etc., are known, the local time-averaged stoichiometry  $\phi$  can be estimated.



The first runs appeared to show large variations in  $\varphi$ . Eventually, we came to believe that these variations were real. As documentation, figure XII-4 shows the results of repeated horizontal traverses with the probe. The data point with error bars is not part of the data but indicates the error bar accuracy of the data. Figures XII-5 and XII-6 show how the nonuniformity in  $\varphi$  persists downstream. We have measured significant variations in  $\varphi$  at  $Z/D = 5$ , even though the cold-flow cone angle of the spray of the air-assist atomizer intersects the walls of the burner at about  $Z/D = 1$  (see fig. XII-3). Figure XII-7 shows a vertical-traverse measurement of soot concentration at  $Z/D = 1.33$ . The variations in  $\varphi$  across the burner were about a factor of 2; the variations in soot are closer to a factor of 10. Figure XII-8 is a contour map of soot concentration at  $Z/D = 2$ , which shows the same effect.

Our concern with these results arose from two practical considerations. It was apparent that most of the soot was being formed in relatively small volumes of the flow. But there was no obvious reason for the particular locations of the nonuniformities in  $\varphi$  and soot. In addition to these complexities, we found that the type of fuel makes a major difference. Figure XII-9 compares the peak, centerline soot concentration of kerosene (isolated point) and the soot obtained using a blend of benzene and heptane (solid line) to simulate a range of hydrogen concentrations (ref. 2). Pure benzene (7.7-percent hydrogen) has a peak soot concentration some two orders of magnitude greater than that of kerosene (14.4-percent hydrogen).

Our attention next was directed to identifying the causes of the observed nonuniformities in  $\varphi$  and soot and then eliminating them. The observed nonuniformities are probably due to the aerodynamic wakes of the fittings on the injector that are upstream of the swirl vanes. Although cold-flow estimates indicate that these wakes are not likely to be important downstream of the swirl vanes, the large density differences associated with the combustion process can combine with the radial pressure gradient associated with swirl to greatly amplify these nonuniformities.

We modified the apparatus by placing the upstream parts and fittings in a larger, low-velocity duct (fig. XII-10). In addition, a tank was added so that we could evaporate fuel in it so as to run the same premixed fuel that is normally run through the injector. In such an experiment, the mass flows of fuel and air and the geometry of the flow remain unchanged.

A better traverse was built into this apparatus so that more-detailed contour maps of  $\phi$  against  $r/D$  and  $\theta$  could be easily measured (fig. XII-11). Figure XII-12 shows the resulting distribution of  $\phi$  - essentially  $\phi$  is constant over cross sections of the burner. This result should be compared with figures XII-4, XII-5, and XII-6, which show large variations in  $\phi$  far downstream of the injector.

Figure XII-13 shows how these changes affect the amount of soot produced. The upper curve is for the original design (fig. XII-2). The fuel is benzene, and the points are the maximum amounts of soot in the burner, which occur around  $Z/D = 2$ . The next lower curve shows the same maximum amounts of soot in a geometry that is described by figure XII-10 and in which the upstream flow was cleared up. This same geometry has the capability of premixed operation. The lowest curve shows that virtually no soot ( $\pm 1$  mg soot/ $m^3$ ) is produced in the premixed flow. In this flow, the mass flows of air both through the air-assist atomizer and through the swirler are the same as when the fuel goes through the injector. The only difference is that the premixed fuel plus air flows through the swirler blades. Hence, the turbulent mixing processes should be very similar in all three cases.

## CONCLUSIONS

Some general trends in soot formation in a turbulent, swirling flow are suggested by the data presented. First, figure XII-9 shows that fuel composition makes a major difference in the amount of soot formed. This is consistent with other work (ref. 3). Second, small changes in upstream geometry apparently can make large changes in soot concentration. Third, as others have found, running lean reduces the amount of soot formed (ref. 4).

Although not shown in a figure, our data from the original design agree quite well with MacFarlane's data (ref. 5) up to 6 atmospheres. But it is not

known if the effects of upstream geometry on soot formation remain the same as the pressure level is raised, and all the data reported here are for an atmospheric pressure burner.

From a practical point of view, the engine designer may not be able to use "clean" fuels. However, our results hint at the possibility of substantial improvements in performance with fuels having a lower percentage of hydrogen in the blend than current practice by means of improved aerodynamic design of the combustor.

#### REFERENCES

1. Prado, G. P.; et al.: Soot and Hydrocarbon Formation in a Turbulent Diffusion Flame. Presented at the 16th Symposium (International) on Combustion, (Cambridge, Mass.), Aug. 15-21, 1976.
2. Shamsavari, Kamren: Measurement of Soot in a Turbulent Diffusion Flame. M.S. Thesis, MIT, 1976.
3. Schirmer, R. M.: Effect of Fuel Composition on Particulate Emission from Gas Turbine Engines. Emissions From Continuous Combustion Systems, Walter Cornelius and William G. Agnew, eds., Plenum Press, 1972, pp. 189-208.
4. Grobman, Jack and Ingebo, Robert D.: Jet Engine Exhaust Emissions of High-Altitude Commercial Aircraft Projected to 1990. NASA TM X-3007.
5. Holderness, F. H.; and MacFarlane, J. J.: Soot Formation in Rich Kerosene Flames at High Pressure. Atmospheric Pollution by Aircraft Engines. AGARD CP-125, 1973, pp. 18-1 to 18-9.



### WATER-FLUSHED SOOT SAMPLING PROBE

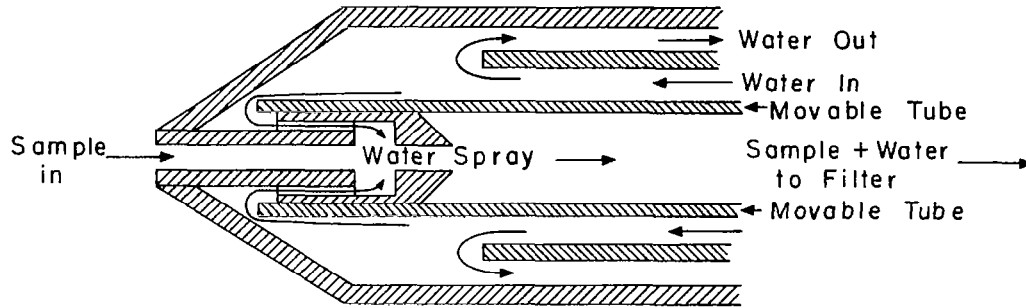


Figure XII-1.

### TURBULENT DIFFUSION FLAME BURNER

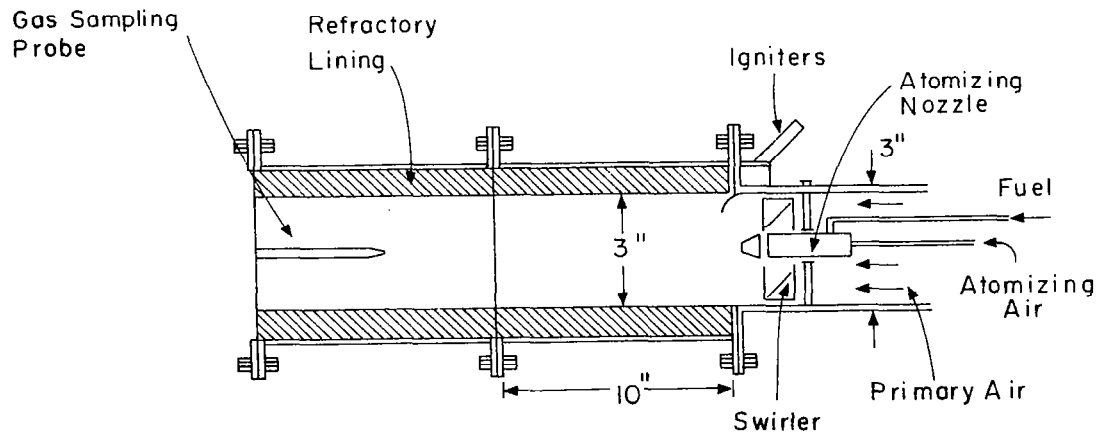


Figure XII-2.

## EXPERIMENTAL METHOD

### PROBE

1. Water-flushed soot sampling probe.
  - a. Water spray is zero for gas analysis.
  - b. Water spray is mixed with gas sample to insure accurate soot collection.
  - c. Water spray rate is controlled by moving inner tube.

### SAMPLING

1. Probe is located inside burner. Information as per  $r$ ,  $\theta$ , and  $z$  obtained from traversing mechanism.
2. Gas sample is drawn through tube.
  - a. For  $\phi$  experiments, sample is sent to gas sampling cart where  $[\text{NO}_x]$ ,  $[\text{HC}]$ ,  $[\text{O}_2]$ ,  $[\text{CO}_2]$ , and  $[\text{CO}]$  can be obtained.
  - b. For soot experiments, sample is pumped through a glass wool filter and wet test meter.

### COORDINATES

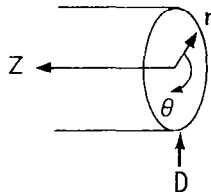


Figure XII-3.

### REPEATABILITY OF NONUNIFORMITY IN EQUIVALENCE RATIO

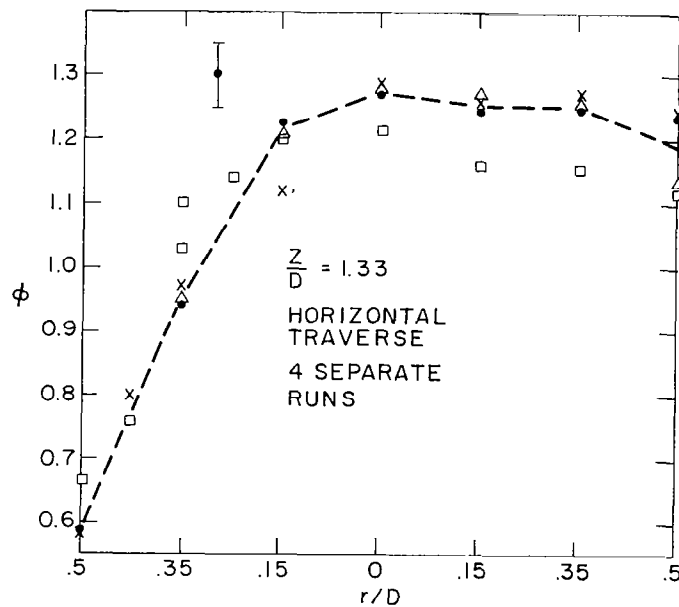


Figure XII-4.



CONTOUR MAP OF EQUIVALENCE RATIO

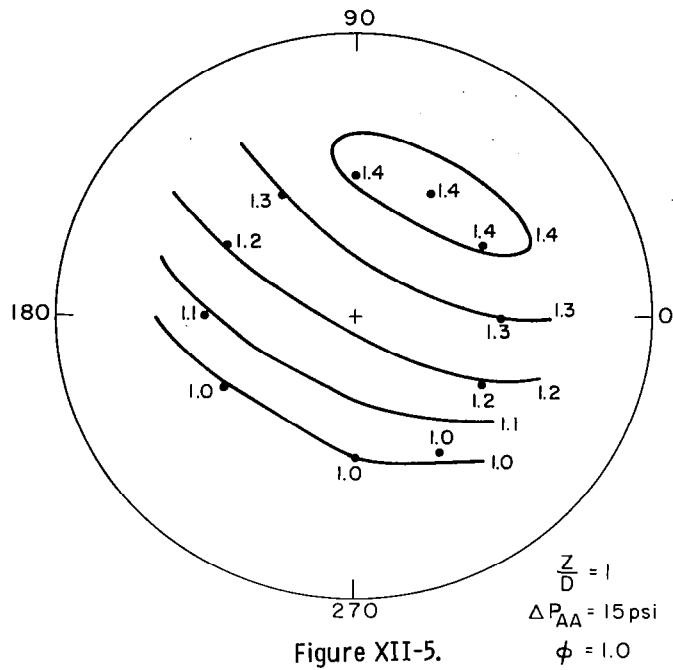


Figure XII-5.

CONTOUR MAP OF EQUIVALENCE RATIO

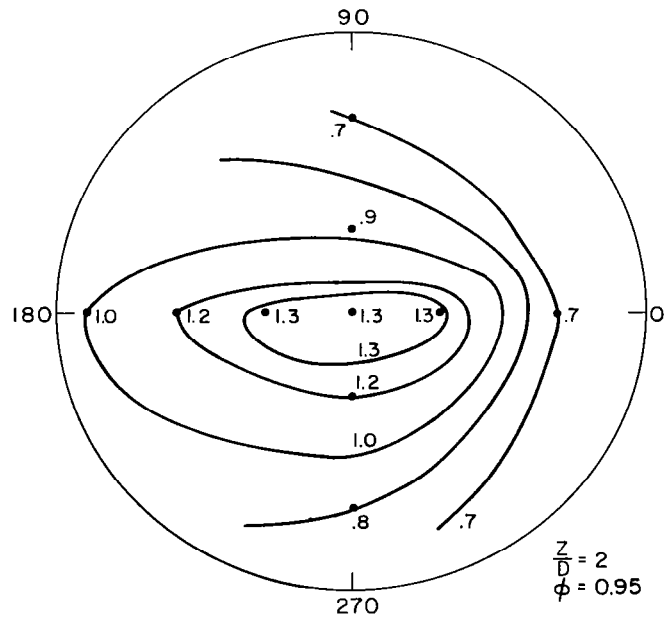


Figure XII-6.

### MEASUREMENTS OF SOOT GRADIENTS

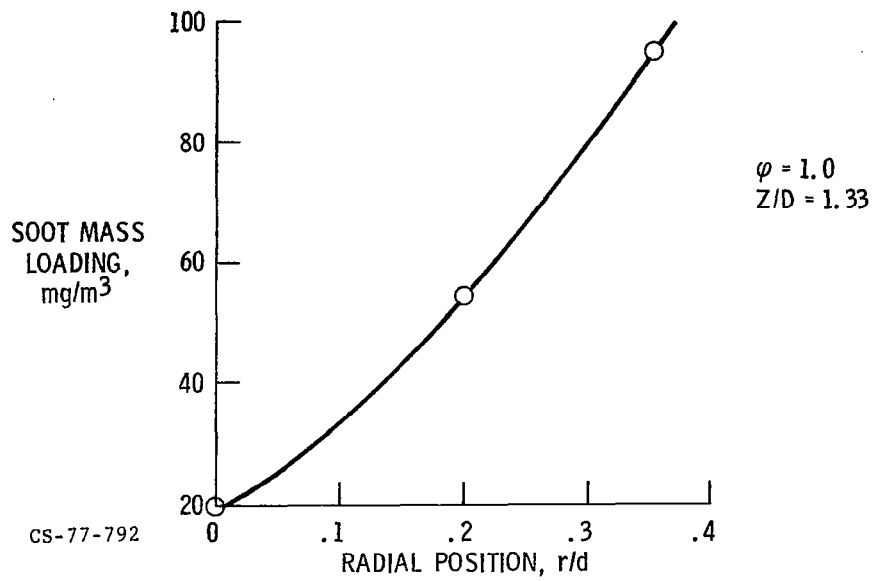


Figure XII-7.

### CONTOUR MAP OF SOOT CONCENTRATION

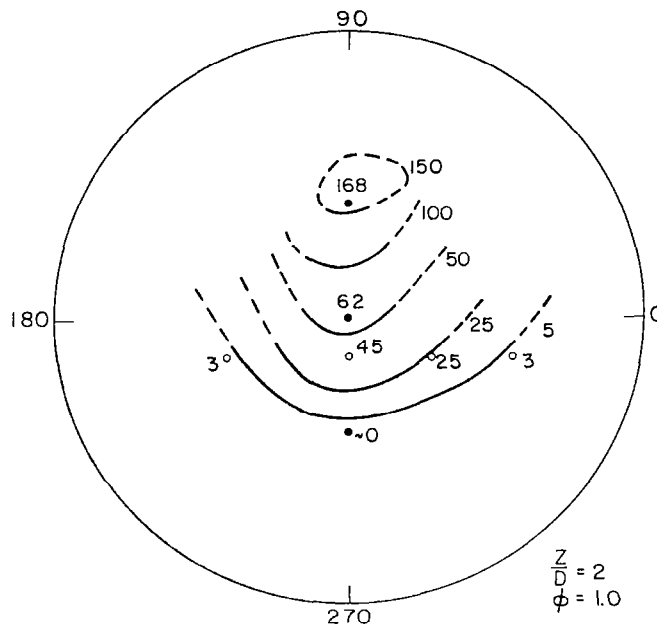


Figure XII-8.

# EFFECT OF HYDROGEN ON PEAK SOOT CONCENTRATION

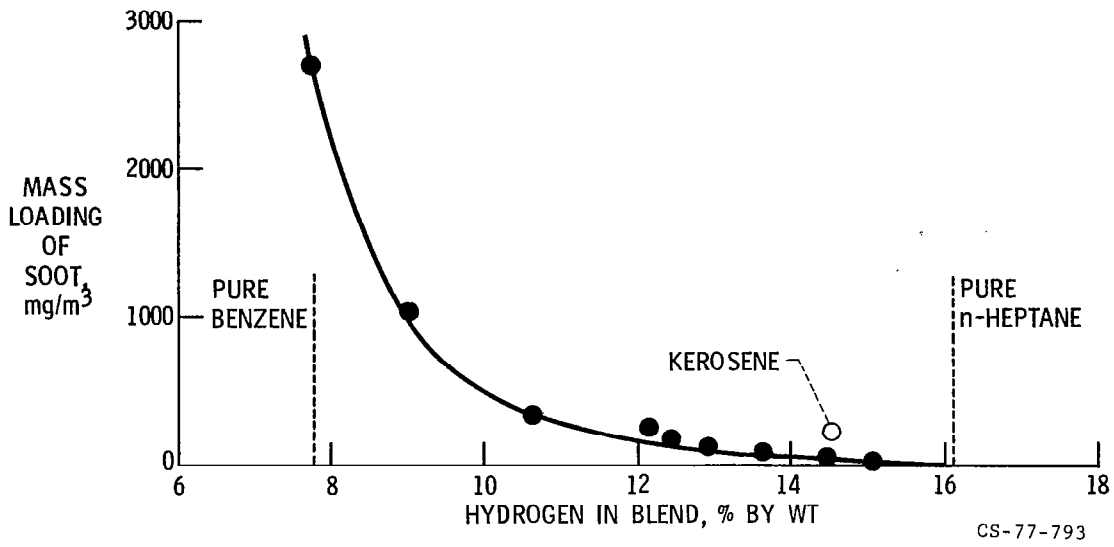


Figure XII-9.

## FLOW SCHEMATIC

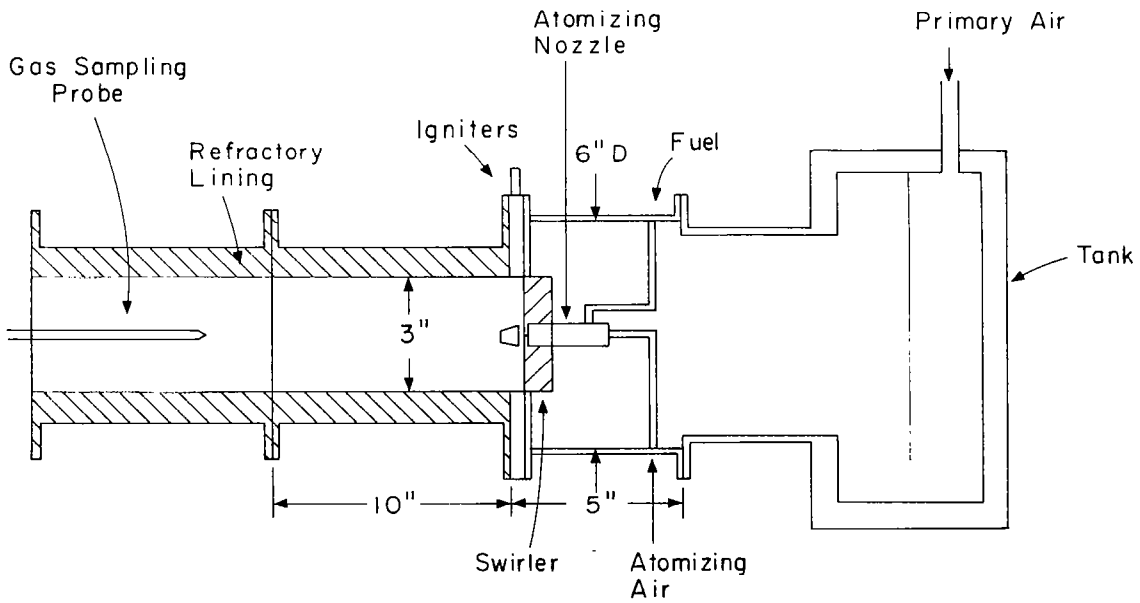


Figure XII-10.

# EXPERIMENTAL LAY-OUT

Probe Positioner

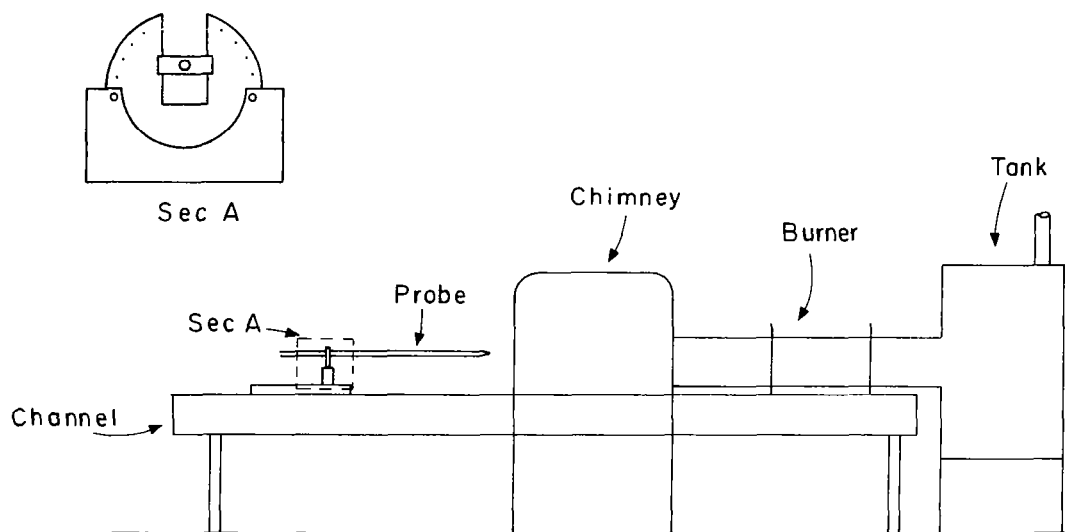
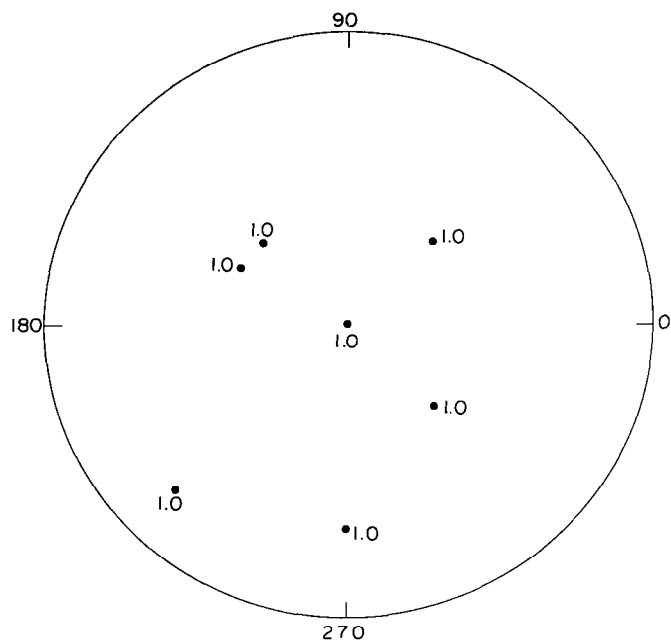


Figure XII-11.

## CONTOUR MAP OF EQUIVALENCE RATIO WITH NEW GEOMETRY



$$\frac{Z}{D} = 2$$

$$\phi = 1 \quad \text{Air} > 68.5 \frac{\text{t}}{\text{hr}}$$

$$\text{Fuel} = 4.6 \frac{\text{t}}{\text{hr}}$$

Figure XII-12.

COMPARISON OF PEAK SOOT CONCENTRATION WITH  
METHOD OF FUEL INTRODUCTION

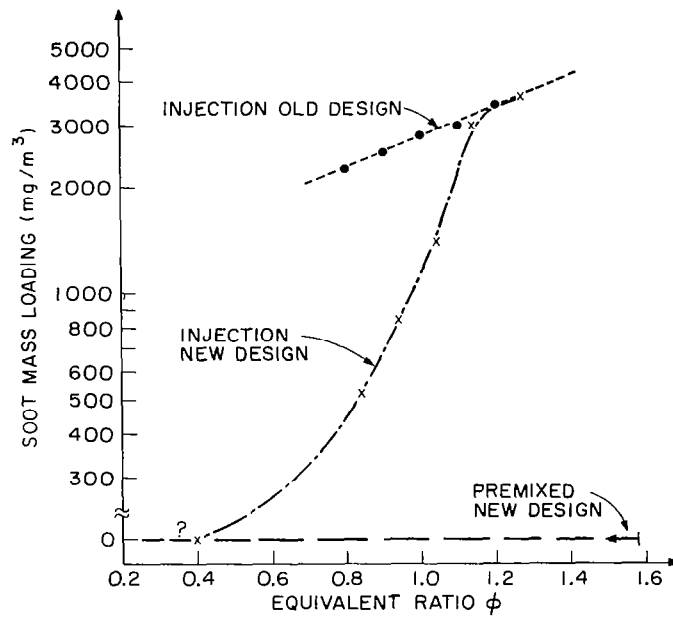


Figure XII-13.